

# Energy & Environmental Science

Accepted Manuscript



This is an *Accepted Manuscript*, which has been through the Royal Society of Chemistry peer review process and has been accepted for publication.

*Accepted Manuscripts* are published online shortly after acceptance, before technical editing, formatting and proof reading. Using this free service, authors can make their results available to the community, in citable form, before we publish the edited article. We will replace this *Accepted Manuscript* with the edited and formatted *Advance Article* as soon as it is available.

You can find more information about *Accepted Manuscripts* in the [Information for Authors](#).

Please note that technical editing may introduce minor changes to the text and/or graphics, which may alter content. The journal's standard [Terms & Conditions](#) and the [Ethical guidelines](#) still apply. In no event shall the Royal Society of Chemistry be held responsible for any errors or omissions in this *Accepted Manuscript* or any consequences arising from the use of any information it contains.

## ARTICLE

# Results of a 20,000 h Lifetime Test of a 7 kW Direct Methanol Fuel Cell (DMFC) Hybrid System - Degradation of the DMFC Stack and the Energy Storage

Cite this: DOI: 10.1039/x0xx00000x

Received 00th January 2012,

Accepted 00th January 2012

DOI: 10.1039/x0xx00000x

www.rsc.org/

N. Kimiaie<sup>\*a</sup>, K. Wedlich<sup>a</sup>; M. Hehemann<sup>a</sup>, R. Lambertz<sup>a</sup>, M. Müller<sup>a</sup>, C. Korte<sup>a</sup>, D. Stolten<sup>ab</sup>

With a proven life of 20,000 operation hours in a lifetime test with a realistic dynamic load profile, the direct methanol fuel cell (DMFC) system V3.3-2 represents a milestone for the commercialization of DMFC systems. The hybrid DMFC system V3.3-2 comprises an in active serial connected 1.0 kW DMFC system and a 45 Ah lithium-ion high-power battery pack. This hybrid system replaces the battery tray of a class 3 forklift truck and can supply a peak load of 7 kW. The advantages of this energy-supply module compared to conventional lead-acid batteries are its higher range (24 h use with a 20 L methanol canister instead of 8 h with battery recharging) and its higher availability (a few minutes are required to exchange methanol canisters instead of hours to recharge the battery). However, in order to ensure that use of the DMFC system V3.3-2 is economic, the DMFC stack must have a durability of at least 10,000 h. This publication describes the degradation behavior of the DMFC stack and of the energy storage system during a lifetime test of the DMFC system V3.3-2 with a dynamic load profile of a material handling vehicle. In the first-ever test worldwide lasting 25,600 h, the hybrid system is successfully operated for 20,000 h. Operation for 20,000 hours is equivalent to the life cycle of a vehicle in the material handling sector. The development and validation of the DMFC system V3.3-2 shows that this system is suitable for use in a forklift truck and that it not only meets the economic system requirements for commercialization but goes well beyond them.

## 1 Introduction

The use of direct methanol fuel cells (DMFCs) enables higher ranges and longer availability (shorter charging times) compared to battery-driven devices. Global DMFC activities reflect this<sup>1,2</sup>. Research and development (R&D) work extends from the micro-DMFC<sup>3,4</sup> with a power of a few watts (< 5 W) through portable applications<sup>5,6</sup> to light traction<sup>7,8</sup> with a power in the lower kilowatt class. Progress in DMFC development over the last few years<sup>9</sup>, further applications, and the current state of the art in DMFC development are described in the literature<sup>10-12</sup>.

According to a market analysis commissioned by Forschungszentrum Jülich, DMFCs are economically efficient in class 3 forklift trucks compared to lead-acid batteries. In cooperation with industrial partners Ritter Elektronik GmbH, Jungheinrich AG, ebm-papst Landshut GmbH, and AKG Verwaltungsgesellschaft, IEK-3 at Forschungszentrum Jülich successfully replaced the battery tray of a forklift truck (Jungheinrich ECE 220) with a kilowatt-class DMFC hybrid system (DMFC system V3.3-1). A prerequisite for commercialization is 24-hour operation of the vehicle in three

shifts and a minimum DMFC stack life of 10,000 operation hours (see<sup>13</sup> Fig. 6). The DMFC system V3.3 is developed in order to fulfil these requirements. This system is a hybrid system that can supply a peak load of 7 kW - comprising an in active series-connected 1.0 kW DMFC system and a 45 Ah lithium-ion high-power battery pack.

Global DMFC development focuses on a power range below 100 W for electronic devices and portable applications. Very few DMFC systems have been developed in the power classes of a few hundred watts or kilowatts. Scientists from Korea presented "a direct methanol fuel cell system to power a humanoid robot"<sup>14</sup>. This DMFC system is a 720 W hybrid system equipped with a 400 W DMFC stack and a 200 Wh lithium-ion battery connected in parallel. In the period 2004–2007, Yamaha showcased the prototype two-wheel-drive scooters FC06 Proto, FC-me, and FC-Dii at the Tokyo Motor Show, in which a 1 kW DMFC system is integrated<sup>15-17</sup>. Information is not available on the market introduction or durability of these DMFC prototypes. Today, there are very few commercially available kilowatt-class DMFC systems in the world. IRD Fuel Cells A/S in Denmark produces 800 W DMFC systems<sup>18</sup> and operates these for stationary power supply in

remote areas. IRD guarantees a lifetime of 3,000 h. Oorja Protonics in the USA markets an on-board battery charger for a wide variety of class 3 vehicles in the materials handling industry. Its system is a 1.5 kW DMFC system with an expected lifetime of 3,500–5,000 total operation hours<sup>19</sup>.

The DMFC system V3.3-2 is a further development of the DMFC system V3.3-1, which has a proven life of 3,000 operation hours<sup>13</sup>. The latter stack exhibited a degradation rate of  $52 \mu\text{V h}^{-1}$  at  $0.1 \text{ A cm}^{-2}$ . An in-depth post-mortem analysis clarified the reasons for the high degradation rate<sup>20</sup>. These findings allowed several measures to be implemented in the DMFC system V3.3-2 to improve long-term stability. The DMFC system V3.3-2 – like its predecessor DMFC system V3.3-1 – is subjected to a lifetime test with a dynamic load profile of a material handling vehicle in order to validate the R&D findings.

Usually, lifetime tests are conducted on DMFC single cells, which are operated for between several hundred and a few thousand hours. These tests help to clarify degradation mechanisms<sup>21-27</sup>, to demonstrate the stability of catalysts or membranes<sup>28-30</sup>, to investigate the influence of impurities<sup>31-33</sup>, or to develop strategies to improve the long-term behavior of DMFCs<sup>34, 35</sup>. In the literature, only a few lifetime tests of DMFC hybrid systems are described. Studies exist on DMFC systems for portable applications in the power range below  $100 \text{ W}$ <sup>36, 37</sup>. With the exception of publications on the DMFC system V3.3-1, which underwent lifetime testing for 3,000 h, no publications on the long-term behavior of kilowatt-class DMFC hybrid systems are publicly accessible.

In designing fuel cell hybrid systems, the dimensions of the DMFC stack as well as the selection of a suitable energy storage solution are important<sup>38</sup>. Lithium-ion batteries (LIBs) have a high power and energy density, which makes them well-suited for use in fuel cell hybrid systems. Battery systems with  $\text{LiNi}_{0.8}\text{Co}_{0.15}\text{Al}_{0.05}\text{O}_2$  (NCA) as cathode are used for this purpose because of their high specific capacity. They are the result of a refinement of conventional systems with  $\text{LiCoO}_2$  and  $\text{LiNiO}_2$ , and boast high safety and stability. Graphite is frequently used as anode material.

The lifetime of a DMFC hybrid system does not just depend on the degradation of the DMFC stack but also on the degradation of the battery pack. The degradation of the energy storage system is mainly determined by cycle-life degradation and calendar degradation. At present, degradation tests of cathode materials are mainly conducted on laboratory cells. These are either set up as whole cells or as half cells. Furthermore, such degradation tests usually involve synthetic full cycles<sup>39-42</sup>. In some studies, however, stylized driving cycles have also been used<sup>43</sup>. In addition, tests have also been conducted on calendar-life aged cells<sup>44, 45</sup>. Analyses of whole battery packs do not usually involve real systems but rather models<sup>46-49</sup>. In some studies, the results of single-cell tests are extrapolated to full systems<sup>50</sup>. The degradation behavior of full battery packs is usually characterized based on cycling in synthetic full cycles<sup>51</sup>. This publication describes a part from the degradation behavior of the DMFC stack, the degradation of the energy storage system during a lifetime test of the DMFC hybrid system V3.3-2 with a realistic dynamic load profile of a material handling vehicle.

During the test, the energy supply system for material handling applications is subjected to a realistic dynamic load profile 24 hours a day - every day until end of life. A lifetime of 20,000 operation hours is demonstrated. The lifetime test does not just exert stress on the DMFC stack but also on the lithium-ion

battery. In this publication, the results of a lifetime test of the DMFC hybrid system V3.3-2 are presented. The results are focused on the degradation of the fuel cell and energy storage system.

## 2 Experimental

The lifetime test of the hybrid DMFC system V3.3-2, which is constructed as a prototype, aims to verify and validate the scientific research results. The objectives of this investigation on the overall hybrid energy system can be broken down as following:

- **Control** of the hybrid system with respect to the DMFC stack, the energy storage (battery), the DC/DC converter, water autonomous operation, efficiency and safety.
- **Degradation** behavior of the DMFC stack, the battery and the peripheral components.
- **Efficiency and reliability** of the DMFC stack, the battery, the DC/DC converter and the peripheral components.
- **Chemical analyses** of the impurities in the system and off-gas measurements.

The priority of this publication is to describe the degradation behavior of the DMFC stack and the battery. Other test results are not covered by this publication and will be published at a later date. The following will describe the DMFC system V3.3-2 and its lifetime test in a test rig.

### 2.1 DMFC-System V3.3-2

The DMFC system V3.3-2 is a further development of the DMFC system V3.3-1. The DMFC system V3.3-1 is described in detail by Mergel et al.<sup>13</sup>.

**Table 1:** Comparison of the DMFC systems V3.3-1 and V3.3-2

Components	V3.3-1	V3.3-2
number of cells in the stack	90	88
bipolar plates	natural	cleaned
cathodic flow field	wick	improved wick
MEAs	self-made	commercial
condenser	bonded	welded
<b>Operation conditions</b>		
stack temperature	48-60 °C	55-67 °C
specific air supply	16-26 mL cm <sup>2</sup> min <sup>-1</sup>	6-12 mL cm <sup>2</sup> min <sup>-1</sup>
specific fuel supply	0.3 mL cm <sup>2</sup> min <sup>-1</sup>	0.3 mL cm <sup>2</sup> min <sup>-1</sup>
methanol concentration	0.45-0.95 mol L <sup>-1</sup>	0.3-0.6 mol L <sup>-1</sup>

The main differences between the DMFC system V3.3-2 and that of V3.3-1 are mentioned in Table 1. The stack is constructed of commercially available membrane electrode assemblies (MEAs) and cleaned bipolar plates to minimize impurities. Another stack modification is the improved fixation of the wicks used to transport the water formed at the cathode out of the cell. By this modification it is now possible to run the stack with a lower specific air supply which leads to higher stack temperature level. With respect to the system components, the condenser is fabricated in a way (welded not bonded by adhesives) to ensure that no more impurities could escape from the condenser and enter the anode system<sup>20</sup>. Fig. 1 shows the main components of the DMFC hybrid system for material handling applications. A 1.0 kW DMFC system and a 45 Ah lithium-ion high-power battery pack provide electric power for the drive motor with a peak load of 7 kW.

The fuel cell and the energy storage system are indirectly connected to each other via a DC/DC converter (active series hybrid). The DMFC hybrid system is controlled in such a way that the battery is kept at a constant charge level. A 20 liter methanol cartridge is integrated in the DMFC hybrid system. One such cartridge is sufficient to continuously operate the vehicle in three-shift operation mode, which means at least 24 h of autonomy with one fill. Depending on the electric power produced by the stack, pure methanol is fed from the methanol cartridge into a mixing container. There, the methanol is mixed with water to form a 0.4 – 0.8 molar methanol-water solution. The water which is obtained by using a condenser is fed into the mixing container. The condensing water originated from the chemical reaction at the cathode and from water permeation from the anode to the cathode. The water found at the cathode is removed from the fuel cell via the cathode exhaust air and fed into the condenser. The condenser is cooled with ambient air in order to obtain water for the anode reaction. The condenser is designed to allow the DMFC system to operate with water autonomous operation up to an ambient temperature of 35 °C.

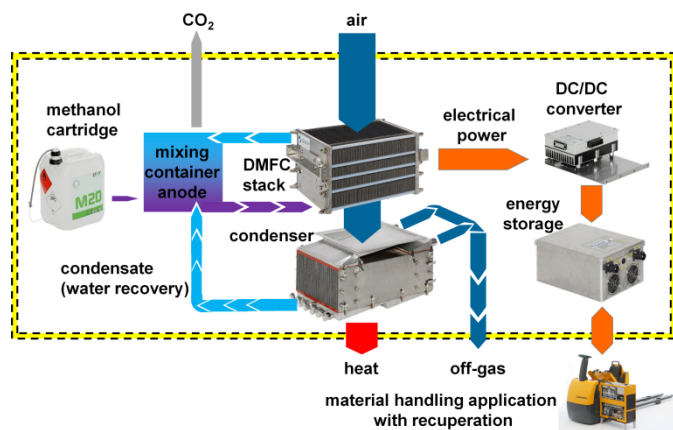


Fig. 1: Main components of the DMFC hybrid system for material handling applications

The DMFC stack in the hybrid system for material handling applications is designed to cover the average base load of 800 W, which is required to supply the peripheral components of the stack and the vehicle's electric motors (drive and lift motors). The DMFC stack is constructed from 88 cells and has a nominal electric power of 1.3 kW. The bipolar plates are developed by Forschungszentrum Jülich GmbH and are fabricated from several layers of expanded graphite. The MEAs used have an active area of 315 cm<sup>2</sup> and are purchased from

Johnson Matthey. According to Johnson Matthey, the catalyst used to fabricate the MEAs is characterized by high corrosion stability<sup>52</sup>. Nafion® N115 from DuPont is used as membrane. The electrode at the anode comprises the catalyst TGP-H-060 loaded with 3.0 mg Pt cm<sup>-2</sup>/1.5 mg Ru cm<sup>-2</sup>. At the cathode, TGP-H-060 is used with a catalyst loading of 1.5 mg Pt cm<sup>-2</sup>. The media supply to the stack is also implemented in the hybrid system. The cathode is supplied with ambient air with the aid of an air blower as a function of stack loading with a specific volume flow rate of 6–12 mL cm<sup>-2</sup> min<sup>-1</sup>. The anode is supplied by a circulation pump, which pumps 0.3–0.6 molar methanol-water solution from the mixing container through the stack with a constant specific volume flow rate of 0.3 mL cm<sup>-2</sup> min<sup>-1</sup>.

The 1 kW DMFC system is hybridized with an energy storage system in order to cover the short-term power peaks of the driving motor, which can be up to 7 kW. Another reason for hybridization is the recuperation of the electrical energy generated by the vehicle when braking, as this cannot be stored in the fuel cell. The energy storage system is designed to ensure that the vehicle could continue to operate for 20 minutes if the DMFC system fails. The hybrid system's energy storage comprises a 45 Ah battery pack with a mean voltage of 26.3 V. This pack contains seven cylindrical cells produced by GAIA connected in series (7s). They are based on LiNi<sub>0.8</sub>Co<sub>0.15</sub>Al<sub>0.05</sub>O<sub>2</sub> cathodes (NCA), organic solvent with LiPF<sub>6</sub> as a conducting salt, and graphite anodes.

## 2.2 DMFC-System V3.3-2

The suitability of the DMFC hybrid energy system for application in a forklift truck is investigated within a lifetime test in a test rig. The test rig has been described in detail in an earlier publication (see<sup>20</sup> Chapter 2.2). In the test rig, the driving profile of a warehouse vehicle in the material handling sector is reproduced. During the lifetime test, the DMFC energy system is subjected to this load profile, which is characteristic of this application. This enables realistic long-term loading of the DMFC hybrid system. Not only the lifting and the driving of the vehicle is reproduced, but so too the recuperation of energy during braking. The DMFC system is not influenced in any other manner by the test rig. The test rig is set up in a hall similar to that of a warehouse and is thus exposed to fluctuations in ambient temperature, air humidity, and dust loads.

The load profile was ascertained during the operation of a Jungheinrich ECE 220 vehicle with the original lead-acid battery (24 V/560 Ah) in a warehouse with a three-shift operation. The vehicle was equipped with measurement techno-

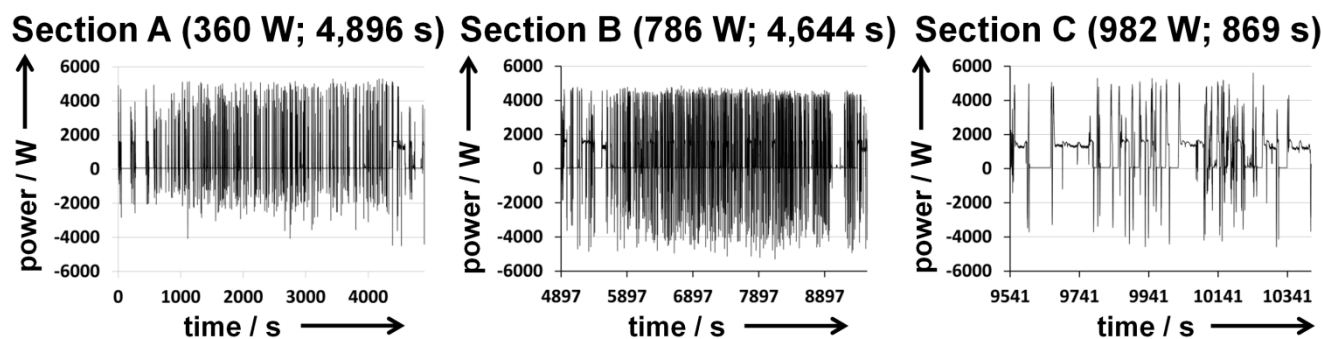


Fig. 2: Sections of the realistic load profile

logy that recorded the battery voltage and electric current over several days. The data revealed that the maximal current under load is approx. 300 A and that recuperation of the braking energy is approx. -200 A when the vehicle braked. When the data is analyzed, three typical blocks of battery loading could be determined<sup>53</sup>. The blocks differ in the average power delivered and in duration. The load profile for the test rig is created by arranging these blocks consecutively one after the other. The load profile can thus be divided into sections A, B, and C (see Fig. 2). Section A (360 W; 4896 s) is a phase of operation with minimal average power characterized by numerous breaks. Section C (982 W; 869 s), in contrast, represents a phase of operation with maximal average power during which long distances are driven. Section B (786 W; 4644 s) reflects characteristic vehicle operation during which the vehicle is used to collect articles from shelves and put them on pallets.

As described in Chapter 2.1, the hybrid system comprises a DMFC stack and a lithium-ion battery. The lifetime test therefore means stressing both the stack and the battery. The test rig is also equipped to allow capacity tests to be performed in order to determine the capacity loss of the battery over time. The lifetime test has to be interrupted for these capacity tests, however, and the test rig has to be re-equipped for the battery tests. The capacity tests are therefore performed on the respective battery pack at irregular intervals with 1 C charge and 1 C discharge rates at room temperature. The packs are initially charged in a constant current phase (CC) to 28.8 V (4.11 V per cell). This is followed by a constant voltage phase (CV) to a current of C/20. The cells are subsequently discharged to 21 V (3 V per cell) without CV. The pack was then charged with CC to 28.8 V and maintained with CV at a current of C/20. Before further operation in the hybrid system, a state of charge (SoC) of 60 % (3.8 V per cell) was established in the battery pack. The cell chemistry offers a charge/discharge window of 4.2 V–2.7 V. It is decided to avoid cycling with 100 % depth of discharge (DoD) to enhance cell life.

For the lifetime test of the energy module in the test rig, methanol is supplied to the DMFC system via 200 L steel drums in order to ensure continuous operation over weekends and on public holidays. The DMFC system is connected to the test rig via the battery plug in the system. The long term test is performed with repeating load profiles by the test rig. All operation parameters, measured data, and error messages are continuously recorded. The measured variables, methanol concentration, methanol volume flow, air mass flow, temperatures and stack and battery voltages are recorded every 2 s. The electric currents from the stack, the battery and at the DC/DC converter are recorded with a sampling frequency of 0.1 s.

The lifetime test of the DMFC system V3.3-2 began in July 2010 and ended in June 2013. The 64 MB of data generated every day gave rise to a total volume of 72 GB for the full test period. These data are analyzed. Selected results are outlined in the following. Further test results will be published at a later date.

### 3 Results and Discussion

The lifetime test of the DMFC system V3.3-2 is characterized by a test duration of almost three years. Large volumes of data are generated and practical experiences are gained during the lifetime test. This publication describes the degradation behavior of the DMFC stack and of the energy storage system

during the lifetime test of the DMFC system V3.3-2 with a dynamic load profile of a material handling vehicle.

#### 3.1 Operation states of the DMFC system V3.3-2

Four operation states can be derived from the lifetime test of the DMFC hybrid system. Fig. 3 shows the progress of the experiment over the test duration time. The operation hours of four operation states are plotted over the test duration. The test duration corresponds to calendar hours and the operation hours to hours during which the DMFC system V3.3-2 is in the respective operation state. The operation state during which the DMFC system V3.3-2 is loaded with the replicated driving profile of the warehouse vehicle in the test rig is referred to as normal operation (black solid line). Downtimes during the lifetime test can be divided into two categories. The first category involves planned downtimes (blue solid line), and the second downtimes due to system failures (blue dashed line), which caused the energy supply module to shut down. Planned downtimes include interruptions to the lifetime test in order to perform capacity tests of the battery, for example, or to conduct maintenance work, undertake modifications to the DMFC hybrid system, or to run another test of the energy supply module. System failures that caused downtimes include cell voltage disturbances, communication problems between the control system and system components, implausible values, and battery faults. The fourth operation state involves modified load cycles (black dashed line). In this operation state, either in the beginning of the test, the hybrid system is loaded with constant, increasing loads (200, 500, 800, 1,000 W) in order to get the energy system into operation. Or later normal operation is reduced to 80 % of the load cycle of the driving profile in order to protect the hybrid system when the control parameters had to be modified. These measures were implemented when the energy supply module was in operation to determine control parameters that counteract the degradation of the stack and the energy storage system.

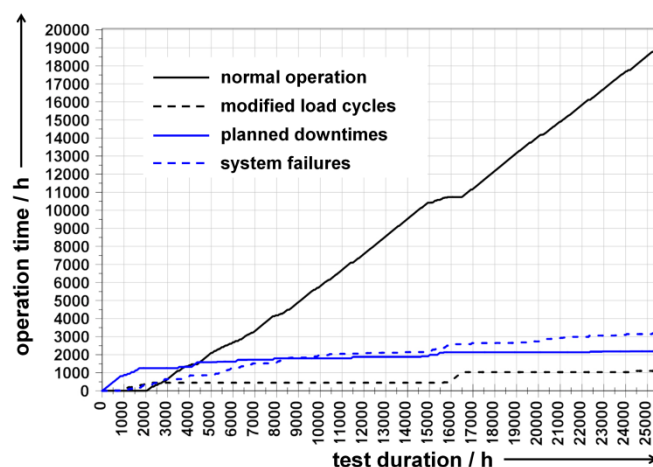


Fig. 3: Operation hours of operational states of the DMFC system V3.3-2 over the duration of the test

Fig. 3 shows that over the test duration of 25,600 hours, the DMFC system V3.3-2 is operated for a total of 20,000 hours in normal operation and modified load cycles. Normal operation within this time accounted about 95 %. The sum total of downtimes during the lifetime test is approx. 5,600 operation

hours. Of these, approx. 2,200 operation hours are planned downtimes, and approx. 3,400 operation hours are downtimes caused by system failures. The planned downtimes over time show that the energy supply module is not in operation for the first approx. 840 hours. The reason for this is the start-up of the energy supply module. The DMFC system V3.3-2 is started up in several steps. First, the control system is programmed, and the functionality and controllability of all system components and sensors are tested. Then, the system components are calibrated in the hybrid system and further measurements are performed to determine relevant variables in the fuel cell system that cannot be measured during operation. These include pressure losses in the anode and cathode supply. Finally, the energy supply module is integrated into a casing with the same dimensions as the vehicle's original battery tray and incorporated into a real vehicle to prove that a real vehicle can be operated with the system.

Following the successful demonstration of the DMFC system V3.3-2 in the vehicle, the energy supply module is mounted in the test rig again. Thereafter, the DMFC hybrid system is operated with a real load profile. This is indicated in Fig. 3 by an inclination of the line for normal operation. A simultaneous increase in the planned downtimes is also visible. This increase emerged because the load profile applied to the energy supply module is not yet run for 24 h, as envisaged in a three-shift operation. This phase of the test is used to optimize the numerous control parameters of the DMFC system during normal working hours of scientific personnel (Monday to Friday, 8 h). After the DMFC system V3.3-2 had been operated for a period of several hundred hours in a single-shift system with no downtimes caused by system failures (reflected by the fact that the line for downtimes due to system failures no longer inclines), the load cycle in three-shift operation is applied to the energy supply module, i.e. 24 h per day and 7 days per week. This is shown by the planned downtime line that runs parallel to the x-axis from calendar hour 1,700.

From this time onwards, the DMFC system V3.3-2 is operated continuously in three shifts. The further progression of the operation states is not described in this publication. These details will be published at a later date.

### 3.2 Interaction stack/battery/load profile

Fig. 4 shows - as prescribed by the load profile in order to run through the load cycle once - the representative responses (stack current, stack voltage, and battery voltage) of the DMFC

hybrid system - comprising a DMFC stack and a lithium-ion battery - to the electric power requirements of the vehicle's electric motor at different operation times. Looking at the stack current (0 A) and stack voltage (75 V), load disconnection can be recognized every 30 minutes for the different operation times. This is performed in order to reduce degradation (reversible fraction) of the stack.

Fig. 4 a) shows the response of the DMFC hybrid system after 1,000 operation hours. The battery voltage shows that the battery is kept at a constant voltage on average of 26.3 V by the DMFC stack. The stack is operated dynamically in accordance with the load profile, which is expressed in changes of the stack current and subsequently of the stack voltage. The electric power output of the stack, without accounting for regular load disconnection in dynamic operation, ranges between a minimum of 120 W - which corresponds to the energy consumed by the fuel cell system itself in order to supply the peripheral components - and a maximum of 1,500 W. The corresponding stack voltage is between 40 V and 58 V, and the stack current is between 5 A and 40 A.

The limited dynamics of the DMFC stack and safety shutdowns due to voltage disturbances in single cells are leading in this period to frequent system failures during operation. The control parameters of the hybrid system - which regulate the power output of the stack and the battery - are thus modified to ensure that the stack is operated less dynamically and the battery more dynamically. Fig. 4 b) shows the response of the DMFC hybrid system with the modified control parameters at 10,000 operation hours. The progression of battery voltage over a load cycle shows that the battery voltage is no longer held at a constant voltage on average by the stack. The mean battery voltage is between 23.6 V and 26.3 V. The charge and discharge peaks of the battery are larger than before because the stack is not operated as dynamically. The stack is operated almost constantly (see stack current and stack voltage in Fig. 4 b)). The stack voltage is approx. 39 V at an electric current production of 21 A. The stack is producing an average power of approx. 820 W until the battery voltage reaches its rated value of 26.3 V. After this, the stack has a phase during which less electric power has to be provided. This phase lasted until the actual value of the battery voltage deviated from the rated value and the stack has to provide more energy once again.

Comparing the dynamic load profile to stack and battery voltage reveals that the dynamics of the load profile are covered by the battery. There is little dynamic load on the stack, which covers the base load of the vehicle application of approx. 800 W. Fig. 4 c) shows the response of the DMFC hybrid system at 20,000 operation hours. Compared to 10,000

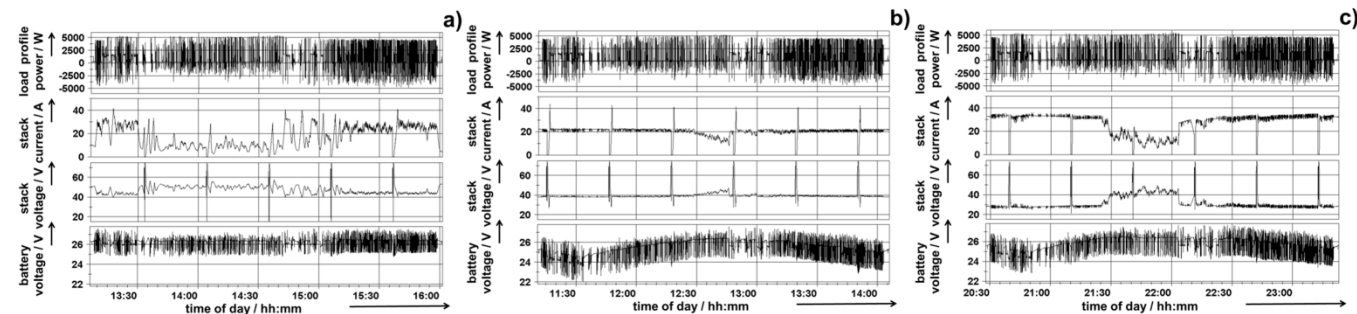


Fig. 4: Response of the DMFC hybrid system (stack current, stack voltage, and battery voltage) for one run through the load cycle to the electric power requirements prescribed by the load profile at different operation times: a) 1,000 operation hours, b) 10,000 operation hours, c) 20,000 operation hours

operation hours previously, the progression of battery voltage is similar; however, it should be noted that the battery is not the same but rather a battery of identical construction (see Chapter 3.4). The load profile data can be used to derive the peak discharge current of the battery to 243 A (5.4 C). According to chapter 2.2 the peak is charge current is 200 A (4.4 C). The average depth of discharge (DoD) is 13 Ah (29 % in relation to 45 Ah). The mean state of charge (SoC) of the battery pack is around 60 % at 26.6 V. The temperature of the cell is between 29 °C and 36 °C.

After 20,000 operation hours, an essential change exists in the behavior of the stack – its operation point altered to higher current output at a lower voltage level (Fig. 4 c)). This can be explained by the degradation of the stack, which is expressed as voltage loss over time (see Chapter 3.3). At a voltage of approx. 32 V and a current of approx. 25.5 A, the power output of the stack is approx. 820 W. The higher power output of the stack leads to the stack having a longer phase during which less electric power has to be provided and the voltage level is higher. For hybrid system operation, in which the DMFC stack is coupled to the lithium-ion battery via a DC/DC converter, the stack voltage plays an essential role. The voltage level of the stack has to be approx. 3 V above the battery voltage value in order to allow the DC/DC converter to convert the stack voltage. This voltage limit is the limiting factor for operation of the hybrid system, and led to the termination of the lifetime test after 25,600 calendar hours.

### 3.3 Degradation of the stack

The operating parameters (air supply, minimal and maximal permissible methanol concentration, and anodic circulation rate) of the stack depend on the electric current produced. They are defined in the control system of the DMFC system V3.3-2. Depending on the load profile, the operation temperature, methanol concentration and stack voltage are adjusted to a certain current. As described above, despite a very dynamic load profile, the stack is operated in an almost constant manner as a result of hybridization with the lithium-ion battery in the DMFC system, where the battery covers the load peaks. During the lifetime test, however, the voltage level of the stack decrease and the electric current produced increase in order to provide the electric power output required by the load profile. The change in stack voltage at a defined specific current density over time is defined as degradation. To determine stack degradation, the continuously recorded measured data of the cell voltages of the stack - which is part of the DMFC hybrid system loaded with the load profile - are filtered at the specific current densities of 50, 75, and 100 mA cm<sup>-2</sup>.

Fig. 5 shows the stack degradation as a mean cell voltage of the stack at the specific current densities of 75 mA cm<sup>-2</sup> (blue) and 100 mA cm<sup>-2</sup> (black) during the operation phases of the stack over the operation time. Operation time means that the stack produces electric current during this time ( $I > 0$  A). The test duration, on the other hand, represents calendar time. This includes both operation hours and system downtimes. System downtimes can be divided into planned interruptions and downtimes caused by system failures (see Chapter 3.1). Looking at both degradation characteristics in Fig. 5, it can be seen that the mean cell voltages are initially scattered. This scattering is caused by the non-constant operation parameters in the stack. In other words, each time the specific current densities are filtered, different stack temperatures, methanol concentrations, and air flow rates are possible. These in turn

depended, as described above, on the load demand of the load profile at the respective point in time.

The progression of both degradation characteristics in Fig. 5 can be divided into 12 sections due to occurring events leading to step in the lifetime test. These sections exhibit regression characteristics for each of the specific current densities in the form of straight lines. The operation hours in each of the sections varies in duration. Table 2 outlines the degradation rate of the stack in the 12 sections for the two different current densities.

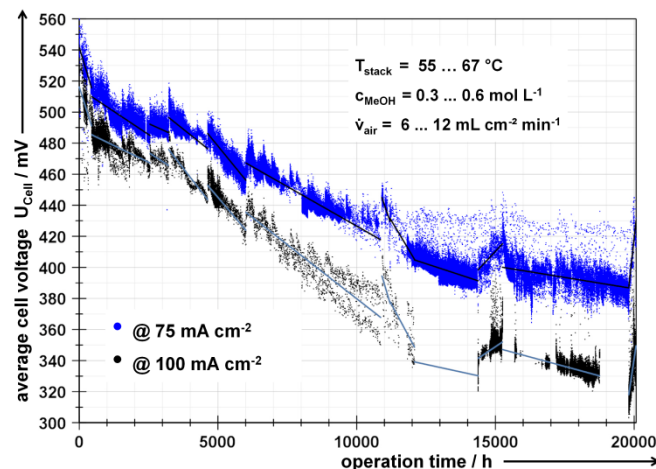


Fig. 5: Graph showing stack degradation in the DMFC system V3.3-2 as voltage loss at a constant current density (filtering of measured data)

Section 1 represents the first 446 operation hours of the stack in the system and shows a degradation rate of 56.4  $\mu\text{Vh}^{-1}$  @ 100 mA cm<sup>-2</sup>. This stack degradation is significant higher than for short stacks with comparable MEAs investigated in test stands. During this period the DMFC system is put into operation by applying constant loads (see Chapter 3.1). It can be assumed that start-up may have caused impurities to be released from the system, which would have led to this degradation rate of the stack. In<sup>20</sup> is the “Influence of Contamination with Inorganic Impurities on the Durability of a 1 kW DMFC System” (DMFC system V3.3-1) described and modifications are suggested to avoid stack degradation in the system. These modifications were implemented in the DMFC system V3.3-2. Despite great care and cleaning of the stack and system components, it cannot be guaranteed that there are no more impurities in the system. For these reasons, section 1 is excluded from the evaluation of the overall degradation rate of the stack during forklift operation.

Section 2 begins by applying the realistic load profile and ends after 2,549 operation hours, because of a capacity test of the energy storage (see Chapter 3.4). During this phase – as described in Chapter 3.1 – the DMFC system is started, which often caused system failures leading to system downtime before constant and stable DMFC operation with the realistic load profile is possible. The degradation rate in section 2 is 11.9  $\mu\text{V h}^{-1}$  @ 75 mA cm<sup>-2</sup> and 8.6  $\mu\text{V h}^{-1}$  @ 100 mA cm<sup>-2</sup>. Comparing the degradation rates @ 100 mA cm<sup>-2</sup> from sections 1 and 2 reveals that the degradation rate dropped by a factor of 6.6. This can be explained by the fact that the amount of impurities decreased by water change.

After 3,226 operation hours (section 3) a leakage between the mixing container of the anode loop and the DMFC stack

occurs. This event is leading to a comprehensive maintenance, where the sealing and the filters are replaced and the water in the system is changed.

Due to the water changing, section 4 starts with a approx. 10 mV higher average cell voltage than at the end of section 3. After 4,627 operation hours, the corrosion of two tie rods, which are used to tension the stack, lead to an electrical short circuit of the stack, which in turn prompted revision of the DMFC stack and system (water change). Looking at the beginning of section 5 it does not seem that the electrical short circuit may prove damaging to the stack, because the average cell voltage is here higher than at the end of section 4.

At the end of section 5 (6,005 operation hours) another water change is carried out. This leads once again to higher average cell voltage at a certain current density, like it can be seen in the beginning of section 6 (see also beginning sections 7 and 10). Water changing removes concentrated impurities in the anodic loop and in this way performance losses can be recovered (reversible degradation).

**Table 2:** Degradation rates in the different sections of the degradation characteristics

Section	Operation time	Degradation rate @	
		75 mA cm <sup>-2</sup>	100 mA cm <sup>-2</sup>
1	0 - 446 h	58.5 μV h <sup>-1</sup>	56.4 μV h <sup>-1</sup>
2	446 - 2,549 h	11.9 μV h <sup>-1</sup>	8.6 μV h <sup>-1</sup>
3	2,549 - 3,226 h	8.0 μV h <sup>-1</sup>	11.6 μV h <sup>-1</sup>
4	3,226 - 4,627 h	14.3 μV h <sup>-1</sup>	23.0 μV h <sup>-1</sup>
5	4,627 - 6,005 h	21.9 μV h <sup>-1</sup>	21.0 μV h <sup>-1</sup>
6	6,005 - 10,907 h	10.2 μV h <sup>-1</sup>	13.9 μV h <sup>-1</sup>
7	10,907 - 11,208 h	51.3 μV h <sup>-1</sup>	60.0 μV h <sup>-1</sup>
8	11,208 - 12,083 h	30.0 μV h <sup>-1</sup>	33.3 μV h <sup>-1</sup>
9	12,083 - 14,376 h	5.9 μV h <sup>-1</sup>	3.9 μV h <sup>-1</sup>
10	14,376 - 15,254 h	-19.1 μV h <sup>-1</sup>	-12.0 μV h <sup>-1</sup>
11	15,254 - 19,807 h	2.9 μV h <sup>-1</sup>	4.8 μV h <sup>-1</sup>
12	19,807 - 20,068 h	-164.4 μV h <sup>-1</sup>	-120.4 μV h <sup>-1</sup>
2 - 12	446 - 20,068 h	7.5 μV h <sup>-1</sup>	8.5 μV h <sup>-1</sup>

The DMFC system could be stably operated nearly 5,000 operation hours during section 6 and shows here a degradation rate of 10.2 μV h<sup>-1</sup> @ 75 mA cm<sup>-2</sup> and 13.9 μV h<sup>-1</sup> @ 100 mA cm<sup>-2</sup>. At the end of section 6 a planned comprehensive maintenance is carried out by changing the filters and the water of the system- with the above mentioned result.

Section 7 ends after 11,208 operation hours when an electrical short circuit due to corrosion of the endplates of the stack lead to considerable system failures, and measures had to be implemented to correct these malfunctions. During the malfunction the stack shows an abnormal degradation rate of 51.3 μV h<sup>-1</sup> @ 75 mA cm<sup>-2</sup> and 60.0 μV h<sup>-1</sup> @ 100 mA cm<sup>-2</sup>. During section 8 the realistic load cycle of the material handling application is partly reduced to 80 % in order to modify the control parameters to counteract the stack damage. The operation parameters of the DMFC system are initially modified in order to re-establish stable system operation after the damage that occurred. For this purpose, the parameter  $U_{\text{Stack\_min}}$  was decreased in the control system to allow the stack produce more electric power. The parameter  $U_{\text{Stack\_min}}$  limits the power load on the stack, i.e. the stack voltage may not exceed this defined minimal limit during the production of electric current. Reducing  $U_{\text{Stack\_min}}$  means that the stack could once again supply sufficient electric power for the driving profile of the forklift truck. These measures are done from section 8 up to section 12, which reveals to different degradation rates.

Especially remarkable are the degradation rates in section 10 and 12 which are negative. This means that there is a performance recovery of the stack. During sections 10 and 12  $U_{\text{Stack\_min}}$  has its minimum value in comparison to the other sections. This means a maximum of current and a response characteristic like shown in Fig. 4 c). However, the higher loading of the stack in the system should be measured in short-stacks to reproduce this result and find an explanation for this behavior, because normally higher loading also expects higher degradation rates.

The lifetime test not only subjected the MEAs to loading but also the bipolar plates and the interfaces between the stack and the system. During the course of the lifetime test, it is found that the stack did not remain permanently tight: leaks emerged in the stack itself and the seals between the stack and the system components also leaked. These leaks lead to a loss of methanol-water solution in the anode loop. This means that it is no longer possible to operate the system with water self-sufficiency since section 8. In other words, additional water is fed into the system via the test rig in order to be able to continue the lifetime test. This problem also affects the methanol supply to the DMFC system, which is reflected in higher methanol consumption in the DMFC system.

Section 12 runs until the lifetime test is terminated. In order to operate the DMFC hybrid system, the stack must provide a voltage of at least 29.3 V. These comprise the battery voltage of 26.3 V and a minimum value of 3 V depending on the DC/DC converter. This stack voltage limit is reached after approx. 20,070 hours of real DMFC system operation. Comparing the progression of the degradation characteristics in section 9 @ 100 mA cm<sup>-2</sup> to the degradation characteristics @ 75 mA cm<sup>-2</sup> in Fig. 5 reveals that the stack failed to achieve a current density of 100 mA cm<sup>-2</sup> for several thousand hours. During the lifetime test, however, measures are implemented in the DMFC system to improve the performance of the stack. These measures are not dealt with in this publication and will be published at a later date. The degradation rates in the sections 9-12 are lower than the degradation rates of the other sections. This can be explained by the additional fresh water that is fed into the system from an external source to compensate for the water volume lost due to leaks. This reduces the concentration of impurities in the DMFC system caused by water recovery. The impacts of selected impurities and the sources of impurities in the system can be found in<sup>20</sup>, where the DMFC system V3.3-1 is used as an example.

The degradation rate for the entire time of operation (sections 2–12) is 8.5 μV h<sup>-1</sup> @ 100 mA cm<sup>-2</sup> when a regression line is formed (not shown in Fig. 5). This value is confirmed by the characterization at the beginning and end of life for defined operation conditions of the stack. The characterization curves at the beginning of life (BoL) and end of life (EoL) are plotted in Fig. 6. The graph shows the mean cell voltage (primary axis – blue) of the cells in the stack and the specific power density (secondary axis – black) versus the current density to facilitate comparison of the characteristics with other stacks or single cells. These characteristics are recorded in a separate test rig for stack characterization before the stack is integrated into the DMFC system and after the stack is removed from the system. At the anode, the stack is kept at a temperature of 70 °C and supplied with a 0.8 molar methanol-water solution. The specific volume flow rate of the anode solution is 0.3 mL cm<sup>-2</sup> min<sup>-1</sup>. The stack is supplied with oxygen with the aid of ambient air, which is neither heated nor humidified. It is fed into the stack with a specific volume flow rate of 30 mL cm<sup>-2</sup> min<sup>-1</sup>.

The start time of the stack is defined as that point in time when the stack is supplied with a methanol-water solution for the first time. Only calendar time is considered, i.e. no differentiation is made between operation hours and downtimes. The BoL of the stack started after running in using a dedicated test rig. When the stack is being run in, U/I characteristics are recorded under defined operation conditions until the stack exhibits stable operation behavior. For the stack integrated in the DMFC system V3.3-2, this occurred after approx. 193 calendar hours. At this time, the U/I characteristics are also recorded to characterize the BoL. The EoL of the stack always depends on the application. The lifetime test is terminated, as mentioned above, because the stack is no longer consistently able to achieve a sufficient voltage level to meet the power requirements prescribed by the DC/DC-converter. A number of subsequent investigations are performed on the DMFC system before the stack is mounted in the test rig for final characterization. The final characterization is performed after approx. 29,237 calendar hours.

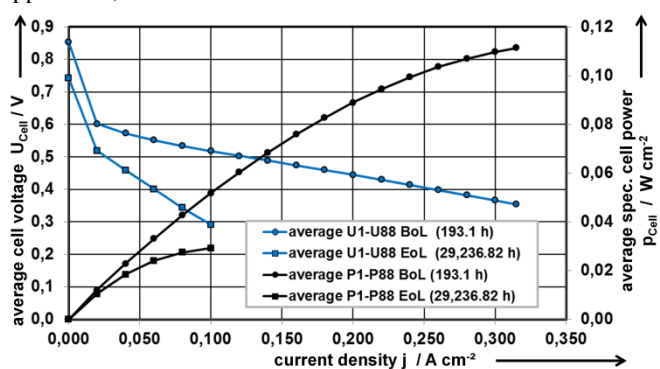


Fig. 6: Comparison of the characterization of stack MM-44 (DMFC system V3.3-2) at BoL and EoL in the test rig

Fig. 6 shows that at BoL (circular shapes), the cells in the stack at  $315 \text{ mA cm}^{-2}$  had a mean cell voltage (blue line) of  $354 \text{ mV}$  and a power density (black line) of  $111 \text{ mW cm}^{-2}$ . Furthermore, the progression of the mean cell voltage and the power density show that the stack did not reach its maximum performance. This is due to the fact the electronic load in the test rig can consume a maximal current of  $100 \text{ A}$ , thus limiting the characterization. If we assume the characteristic variables at BoL @  $100 \text{ mA cm}^{-2}$ , then the mean cell voltage is  $518 \text{ mV}$  and the power density  $52 \text{ mW cm}^{-2}$ .

EoL (square shapes) in Fig. 6 shows that the stack can only be loaded with a maximal current density of  $100 \text{ mA cm}^{-2}$ . The reason for this is that when a load of  $120 \text{ mA cm}^{-2}$  is applied, single cells in the stack exhibit a cell voltage of less than  $100 \text{ mV}$ , which leads to a safety shutdown in the test rig. This in turn limits characterization to the lower range. After 29,237 calendar hours, the cells in the stack @  $100 \text{ mA cm}^{-2}$  had a mean cell voltage of  $292 \text{ mV}$  and a power density of  $29 \text{ mW cm}^{-2}$ . Compared to BoL, this represents a voltage loss of  $226 \text{ mV}$  over a period of 29,044 calendar hours. The degradation rate of the stack can thus be calculated as  $7.8 \mu\text{V h}^{-1}$ . Compared to the degradation rate of  $8.5 \mu\text{V h}^{-1}$ , which is derived from the regression line of data filtering and the operation hours for sections 2–12 (see Table 2), the following can be concluded: first, degradation rates can be determined using data filtering. The deviation of less than 10 % in the degradation rate is due to the different operation conditions of the stack in the DMFC system and in the test rig. Second, stack degradation is caused by operation the stack in the system and not by downtimes

during which the stack is shutdown in a defined state in the DMFC system.

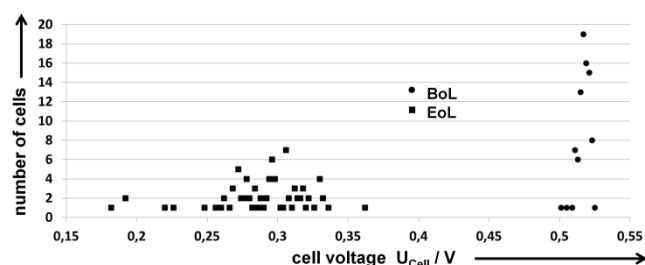


Fig. 7: Comparison of cell voltage distribution @  $100 \text{ mA cm}^{-2}$  of the DMFC stacks MM-44 at BoL and EoL

Fig. 5 shows that the scattering of the data increases with the operation time. The increased scattering, however, cannot be explained by the operation parameters. It must be caused by an effect related to the degradation of the MEAs in the stack. Fig. 7 compares the cell voltage distribution @  $100 \text{ mA cm}^{-2}$  of the DMFC stack MM-44 in the DMFC system V3.3-2 at BoL (dots) and EoL (squares). The number of cells is plotted against the cell voltage. Examining the cell voltages at BoL, it becomes clear that the frequency distribution of the cell voltages ranges between  $502 \text{ mV}$  and  $525 \text{ mV}$ , which reflect a high stack quality. At EoL, the values range from  $184 \text{ mV}$  to  $362 \text{ mV}$ . This indicates that the MEAs in the stack degrade differently. These different degradation rates of the MEAs in the stack should be investigated in a post-mortem analysis of the stack.

### 3.4 Degradation of the energy storage system

Chapter 3.2 describes how the energy storage system in the DMFC hybrid system V3.3-2 is cycled using real load cycles of a forklift truck. In this chapter, the relevant battery data recorded over a period of four years are evaluated. During the lifetime test, problems arose with the CAN bus communication between the energy storage system and system control, which means that two identical lithium-ion battery packs are operated alternately and subjected to capacity tests. These are termed GAIA II and GAIA III. A third battery pack GAIA I is used as a reference and subjected mainly to calendar-life degradation. Table 3 details the capacity tests of the two GAIA batteries used.

The battery GAIA III is integrated into the DMFC system V3.3-2 around four months after the beginning of the lifetime test and the hybrid system putting into operation. It achieves a total of 12,514 operation hours throughout the different installation phases. When the GAIA III malfunctioned in the hybrid system, the battery GAIA II – which had been used in the DMFC system V3.3-1 too – is used temporarily. GAIA II is used in the DMFC system V3.3-2 for a total of 7,500 operation hours and is used 10,646 operation hours at all.

The degradation of an energy storage system can be determined by analyzing the state of health (SoH). The state of health of a battery is defined as the quotient of capacity at a specific point in time and initial capacity ( $Q_t/Q_0$ )<sup>54</sup>. To determine the degradation of lithium-ion batteries, several factors must be taken into account. Degradation during operation is always affected by calendar life and cycle life<sup>55</sup>. Fig. 8 a) shows the cycle-life degradation of the battery pack used in the lifetime test. The SoH of both battery packs decreases almost linearly

**Table 3:** Overview of capacity tests of the two battery packs used

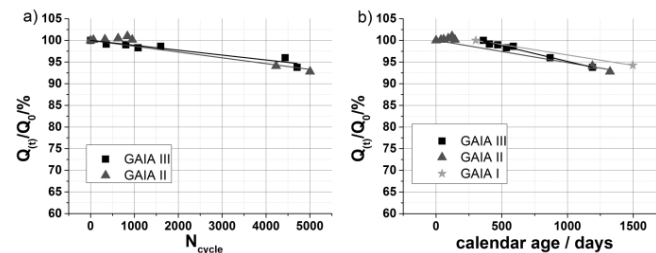
Date	Full cycles	Operation hours	Calendar age [d]	Discharge current [A]	Discharge duration [h]	Energy [Wh]	Capacity [Ah]	State of health SOH [%]
<b>GAIA II:</b>								
19.10.2009	0	0	0	45.4	0.84	977	38.4	100.0
25.11.2009	65	498	37	45.4	0.85	976	38.4	100.13
16.12.2009	327	942	58	45.5	0.85	976	38.5	100.23
20.01.2010	628	1,557	93	45.6	0.85	1,130	38.6	100.5
17.02.2010	838	1,985	121	45.6	0.85	1,149	38.7	100.96
12.03.2010	948	2,225	144	45.6	0.84	969	38.4	100.15
21.01.2013	4,230	9,358	1,190	45.7	0.79	908	36.1	94.09
03.06.2013	5,004	10,646	1,323	45.6	0.78	895	35.6	92.79
<b>GAIA III:</b>								
14.10.2010	0	0	360	46.0	0.85	992	39.1	100
29.11.2010	356	791	406	46.0	0.84	1,066	38.8	99.1
31.01.2011	803	1,785	469	46.1	0.84	1,089	38.7	99.0
07.04.2011	1,084	2,408	535	46.3	0.83	972	38.5	98.3
30.05.2011	1,598	3,474	588	46.2	0.81	971	38.6	98.6
05.03.2012	4,436	9,438	868	46.3	0.81	941	37.6	96.0
21.01.2013	4,709	11,172	1,190	46.5	0.79	922	36.7	93.8
25.05.2013	5,882	12,514	1,314	Heavy self-discharge observed -> For reasons of safety, cap. test no longer possible!				

with the increasing number of cycles. The SoHs of GAIA II and GAIA III show similar behavior. Fig. 8 b) plots the SoHs of the battery packs against calendar age. In addition to the batteries GAIA II and GAIA III, the values for GAIA I are also shown. This pack is used for getting in operation and for the first tests of the DMFC hybrid system. It completed approximately < 100 full cycles. The capacity drop in the case of this battery is mainly determined by calendar life.

Analyzing Fig. 8 a) and b), it can be concluded the following: in relation to full cycles, the SoH of GAIA III after the end of the test is similar to the SoH of GAIA II (SoH (GAIA III, 4,436 full cycles) = 96 % and SoH (GAIA II, 4,230  $N_{\text{cycle}}$ ) = 94 %). The same applied to the dependence on calendar age (SoH (GAIA III, 1,190 days) = 93.8 % and SoH (GAIA II, 1,190 days) = 94.1 %). The battery pack GAIA I is used during the first year to run the DMFC hybrid system V 3.3-1. Within this period, no full capacity tests are performed. For this reason, the initial capacity ( $Q_0$ ) of this battery pack is unknown. The value of the first capacity test performed is thus set to  $Q_0$ . The absolute values of the GAIA I pack therefore cannot be compared to those of the other battery packs. However, the degradation rate during the storage period is very similar to the degradation rate of the other packs.

As the SoHs of GAIA III and II deviated from each other by 2 % after a similar number of full cycles, but their SoHs at the

same calendar age differed only by 0.3 %, degradation of the system described here appears to be predominantly dominated by calendar age. Another indication for this is the behavior of GAIA I whose degradation rate is very similar to that of each of the other packs although its degradation occurred mainly as a result of calendar age.

**Fig. 8:** a) SoH versus full cycles, b) SoH versus calendar age of the battery packs

The discharge curves of the capacity tests of GAIA III are used to extract incremental capacities (ICs), which are shown in Fig. 9. The curves are smoothed for the display. They shift to the left and upwards with an increasing number of cycles. Dubarry et al. refer to an intensity loss of all peaks due to the loss of active material<sup>56</sup>. The shifting of all lines to the left (IR drop)

indicates an increase in the internal resistance of the cells. The increasing IR drop means that the discharging and charging end voltages are reached prematurely, which led to overcharging and under discharging effects<sup>56</sup>.

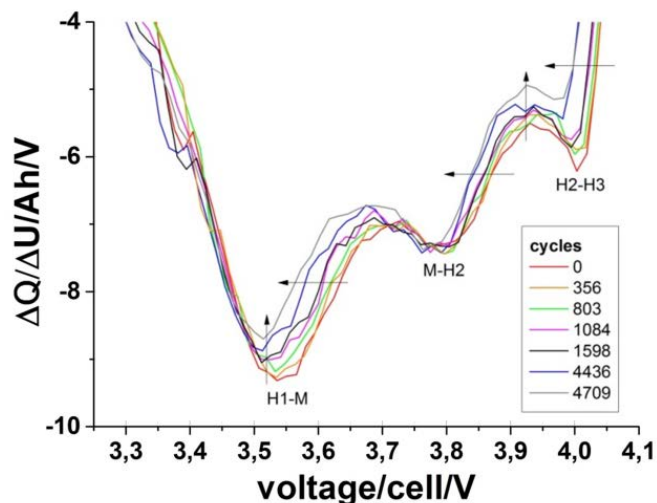


Fig. 9: Incremental capacities of the discharge curves of GAIA III after different full cell cycles

The three peaks in the IC diagram represent the phase transitions for NCA according to Chung et al.<sup>57</sup>. In contrast to the cells described by Chung, the transition of the first hexagonal phase to a monoclinic phase (H1-M) occurred here between 3.5 V and 3.55 V (cf. Chung 3.68 V). The transition of the monoclinic phase to the second hexagonal phase (M-H2) occurred at 3.8 V (cf. Chung 3.94 V) and the transition of the second hexagonal phase to the third hexagonal phase (H2-H3) occurred between 3.95 V and 4 V (cf. Chung 4.15 V). These differences emerged because the battery pack is measured as a whole in the place of single cells. The spectra therefore constitute a superposition of all single cells in the pack. Furthermore, the rate at which the two diagrams are recorded is also different. Chung et al. selected a feed rate of 0.05 mVs<sup>-1</sup> and recording therefore lasted 11 h. In this experiment, the curve is recorded with 1 C. The kinetics also caused the peaks to shift.

After 5,882 full cycles, rapid self-discharge is observed for the GAIA III pack. This pack is subsequently taken apart and the single cells are separated from the in-built battery management system (BMS). The single cell voltages immediately recovered producing approx. 3V. This indicates that the cause of the observed self-discharge is a defect in the battery pack electronics. However, an analysis of the BMS is not part of this work.

#### 4 Conclusion

The hybrid DMFC system V3.3-2 comprises an in active serial connected 1.0 kW DMFC system and a 45 Ah lithium-ion high-power battery pack. This hybrid system replaces the battery tray of a class 3 forklift truck and can supply a peak load of 7 kW. The advantages of this energy-supply module compared to conventional lead-acid batteries are its higher range (24 h use with a 20 L methanol canister instead of 8 h with battery recharging) and its higher availability (a few minutes are required to exchange cartridges instead of hours to recharge the battery). However, in order to ensure that use of the DMFC

system V3.3-2 is economic, the DMFC stack must have a lifetime of 10,000 h at least. R&D at IEK-3 over the last few years has therefore concentrated on identifying measures to improve the long-term stability of DMFC systems. In order to validate R&D results, two prototypes were constructed and subjected to dynamic lifetime testing using real load profiles until end of life (EoL).

The DMFC system V3.3-2 is a further development of the DMFC system V3.3-1, which has been subjected to a durability test for 3,000 hours with a realistic dynamic load profile for material handling applications. The degradation rate of this system amounts to rate of 52  $\mu\text{V h}^{-1}$  at 100 mA cm<sup>2</sup>. As a result of this experiment the causes of the stack degradation were analyzed by an extensive post mortem analysis. The major causes of degradation in the DMFC system V3.3-1 were identified<sup>20</sup>. On the basis of these findings the DMFC V3.3-2 system was modified to improve long-term stability. These modifications concern both stack and system components. In order to minimize the introduction of contaminants a careful choice of materials, cleaning procedures and new manufacturing methods are conducted. At the same time, the modification of the wicks at the cathodic flow field leads to more favorable operation conditions of the stack. Another issue is the use of commercial MEAs with new catalyst materials with improved corrosion resistance of the PtRu catalysts.

The duration of the test using the DMFC system V3.3-2 described here is 25,600 hours. Of this, 20,000 operation hours are demonstrated in the hybrid system. Operation for 20,000 hours is equivalent to the life cycle of a vehicle in the material handling sector. The development and validation of the DMFC system V3.3-2 shows that this system is suitable for use in a forklift truck and that it not only meets the economic system requirements for commercialization but goes well beyond them. This publication focuses on describing the degradation behavior of the DMFC stack and the energy storage system. Other test results are not covered by this publication and will be published at a later date.

The DMFC hybrid system is controlled so that the lithium-ion battery is kept at a mean state of charge (SoC) of 60 % by the DMFC stack. The DMFC stack covers the base load energy required by the application. The peak loads are covered by the battery. The hybridization allows the DMFC stack to be operated in an almost constant manner despite a very dynamic load profile. The stack/battery/load profile interaction showed that the lifetime test of the hybrid system not only means stressing the stack but also the battery.

Over the full period of operation, the DMFC stack exhibits a degradation rate of 8.5  $\mu\text{V h}^{-1}$  @ 100 mA cm<sup>2</sup>. During this period, different degradation rates are determined at different points in time, which are caused by different reasons. At the beginning of the lifetime test, impurities in the DMFC system are probably the reason for a degradation rate of 56.47  $\mu\text{Vh}^{-1}$  @ 100 mA cm<sup>2</sup>. After the impurities in the system diminished, the DMFC stack exhibited a degradation rate that is 6.6 times lower (8.6  $\mu\text{V h}^{-1}$  @ 100 mA cm<sup>2</sup>).

Due to the degradation (voltage loss over operation time) of the stack during the lifetime test, the stack had to produce more electric current in order to provide sufficient power for the application. The increased stress on the stack in turn does not lead automatically to higher degradation rates as assumed. Further investigations have to be done to explain the correlation between current density and degradation rates. During the period when the DMFC system could no longer be operated with water self-sufficiency and extra water had to be fed into

the system, the DMFC stack exhibited its lowest degradation rates. This would be an argument in favor of operation the DMFC system with a methanol-water solution instead of with pure methanol as this would minimize the impurities that accumulate when water is recovered. However, this would also impair the range of the vehicle and thus challenge the vehicle's economic efficiency. For this reason – and with respect to impurities at the beginning of the test phase – future DMFC system developments should comprise on-board ion cleaning. The first steps have already been described by Park et al.<sup>35</sup>

Two lithium-ion high-power GAIA battery packs (45 Ah, 7s, 26.3 V) are operated during the lifetime test. The battery packs are tested for 4 years under realistic loading conditions and they completed 5,000 cycles with a degradation of 6 %. According to the available data for the load profile used, the dimensions of the battery packs, and the resulting charging and discharging strokes, calendar age of the cells appears to be the determining factor for cell degradation. Another decisive factor for the long-term application of such battery packs is the lifetime of the integrated electronics. During the lifetime test, errors occurred in the CAN bus communication and in the battery management system (BMS) but not in the cells. This demonstrates that lithium-ion batteries are well suited for hybridization with fuel cells in highly dynamic applications. However, there is still a need to develop balance-of-plant (BoP) components for battery systems.

With a proven life of 20,000 operation hours in a lifetime test with a realistic dynamic load profile, the DMFC system V3.3-2 represents a milestone for the commercialization of DMFC systems. All in all, the combination of reduced contaminants, more favorable operation conditions and improved catalyst material in comparison to the DMFC system V3.3-1 reduced the degradation rate of the DMFC system V3.3-2 by a factor of about 6. Future R&D projects will look at cutting costs, as well as increasing efficiency and power density.

Further results of the DMFC-System V3.3-2 lifetime test with a focus on efficiency and reliability and analytical results, will be published in upcoming publications.

## Acknowledgements

The development work is funded by the Federal Ministry of Economics and Technology (BMWi) as part of a collaborative project (reference nos. 0327769A and 0327769B).

## List of Symbols

### Latin Letters

A	ampere – measurement unit for electrical current
Al	aluminum – chemical element
B	byte – measurement unit for digital information
BMS	battery management system
BoL	begin of life
c	centi ( $10^{-2}$ ), symbol for concentration
C	coulomb (As) – measurement unit for electrical charge
°C	centigrade – measurement unit for temperature
CC	constant current
Co	cobalt – chemical element
CV	constant voltage
DC	direct current
DMFC	direct methanol fuel cell

DoD	depth of discharge
EoL	end of life
F	fluorine – chemical element
g	gram – measurement unit for mass
G	giga ( $10^9$ )
h	hour – measurement unit for time
I	symbol for current
IC	incremental capacity
IEK-3	Institute of Energy and Climate Research, IEK-3: Electrochemical Process Engineering
IR	internal resistance
j	symbol for current density
k	kilo ( $10^3$ )
L	liter – measurement unit for volume
Li	Lithium – chemical element
LIB	Lithium-ion battery
m	milli ( $10^{-3}$ ), meter – measurement unit for length
M	mega ( $10^6$ )
MEA	membrane electrode assembly
MeOH	methanol
min	minute – measurement unit for time
mol	mole – measurement unit for the amount of chemical substances
NCA	cathodes with Li, Ni, Co and Al-oxide
Ni	Nickel – chemical element
O	oxygen – chemical element
P	phosphorus – chemical element
Pt	platinum – chemical element
Q	symbol for capacity
R&D	research and development
Ru	ruthenium – chemical element
s	second – measurement unit for time, serial connection of cells in batteries
SoC	state of charge
SoH	state of health
T	symbol for temperature
U	symbol for voltage
V	volt – measurement unit for voltage
$\dot{v}$	symbol for specific volume flow
W	watt – measurement unit for power

### Greek Letters

$\mu$	micro ( $10^{-6}$ )
-------	---------------------

### Index

0	initial
(t)	specific point in time

### Notes and references

<sup>a</sup> Forschungszentrum Jülich GmbH, Institute of Energy and Climate Research, IEK-3: Electrochemical Process Engineering, 52425 Jülich,

Germany. E-mail: n.kimiaie@fz-juelich.de; Fax: +49 2461 61 6695; Tel: +49 2461 61 6484

<sup>b</sup> Chair for Fuel Cells, RWTH Aachen University, Germany.

## References

1. A. S. Aricò, S. Srinivasan and V. Antonucci, *Fuel Cells*, 2001, **1**, 133-161.
2. R. Dillon, S. Srinivasan, A. S. Aricò and V. Antonucci, *J. Power Sources*, 2004, **127**, 112-126.
3. S. K. Kamarudin, W. R. W. Daud, S. L. Ho and U. A. Hasran, *J. Power Sources*, 2007, **163**, 743-754.
4. S. Sundarajan, S. I. Allakhverdiev and S. Ramakrishna, *Int. J. Hydrogen Energy*, 2012, **37**, 8765-8786.
5. P. Agnolucci, *Int. J. Hydrogen Energy*, 2007, **32**, 4319-4328.
6. S. K. Kamarudin, F. Achmad and W. R. W. Daud, *Int. J. Hydrogen Energy*, 2009, **34**, 6902-6916.
7. Z. Qi, in *Encyclopedia of Electrochemical Power Sources*, ed. J. Garche, Elsevier, Amsterdam, 2009, pp. 302-312.
8. J. Garche, in *Hydrogen and Fuel Cells - Fundamentals, Technologies and Applications*, ed. D. Stolten, WILEY-VCH Verlag GmbH & Co. KGaA, Weinheim, 2010, ch. 35, pp. 715-732.
9. B. Emonts, L. Blum, T. Grube, W. Lehnert, J. Mergel, M. Müller and R. Peters, in *Fuel Cell Science and Engineering - Materials, Processes, Systems and Technology*, eds. D. Stolten and B. Emonts, Wiley-VCH Verlag GmbH & Co. KGaA, Weinheim, 2012, vol. 1, ch. 1, pp. 3-42.
10. A. S. Aricò, V. Baglio and V. Antonucci, in *Electrocatalysis of Direct Methanol Fuel Cells*, eds. H. Liu and J. Zhang, Wiley-VCH Verlag GmbH & Co. KGaA, Weinheim, 2009, ch. 1, pp. 1-78.
11. J. Mergel, A. Glüsen and C. Wannek, in *Hydrogen Energy*, ed. D. Stolten, Wiley-VCH Verlag GmbH & Co. KGaA, Weinheim, 2010, ch. 3, pp. 41-60.
12. X. Li and A. Faghri, *J. Power Sources*, 2013, **226**, 223-240.
13. J. Mergel, H. Janssen, M. Müller, J. Wilhelm and D. Stolten, *J. Fuel Cell Sci. Technol.*, 2012, **9**, 031011/000001-031011/000010.
14. H.-I. Joh, T. J. Ha, S. Y. Hwang, J.-H. Kim, S.-H. Chae, J. H. Cho, J. Prabhuram, S.-K. Kim, T.-H. Lim, B.-K. Cho, J.-H. Oh, S. H. Moon and H. Y. Ha, *J. Power Sources*, 2010, **195**, 293-298.
15. Yamaha, FC06 Proto, <http://global.yamaha-motor.com/news/2004/0922/dmfc.html>, Accessed December 2013.
16. Yamaha, FC-me, <http://global.yamaha-motor.com/news/2005/1005/tms.html>, Accessed December 2013.
17. Yamaha, FC-Dii, <http://global.yamaha-motor.com/news/2007/1005/tms-mc.html>, Accessed December 2013.
18. IRD Fuel Cells A/S, Direct Methanol Fuel Cell System (DMFC), [http://www.ird.dk/getattachment/60d6608d-fc05-455c-bc36-41dfad5b0345/IRD\\_DMFC.aspx](http://www.ird.dk/getattachment/60d6608d-fc05-455c-bc36-41dfad5b0345/IRD_DMFC.aspx), Accessed December 2013.
19. T. Ramsden, M. Ulsh, S. Sprick, J. Kurtz, and C. Ainscough, Direct Methanol Fuel Cell Material Handling Equipment Deployment, [http://www.hydrogen.energy.gov/pdfs/review12/mt004\\_ramsden\\_2012\\_o.pdf](http://www.hydrogen.energy.gov/pdfs/review12/mt004_ramsden_2012_o.pdf), Accessed December 2013.
20. N. Kimiaie, C. Trappmann, H. Janßen, M. Hehemann, H. Echsler and M. Müller, *Fuel Cells*, 2014, **14**, 64-75.
21. S. D. Knights, K. M. Colbow, J. St-Pierre and D. P. Wilkinson, *J. Power Sources*, 2004, **127**, 127-134.
22. P. Zelenay, *ECS Trans.*, 2006, **1**, 483-495.
23. W. Chen, G. Sun, J. Guo, X. Zhao, S. Yan, J. Tian, S. Tang, Z. Zhou and Q. Xin, *Electrochim. Acta*, 2006, **51**, 2391-2399.
24. M. K. Jeon, J. Y. Won, K. S. Oh, K. R. Lee and S. I. Woo, *Electrochim. Acta*, 2007, **53**, 447-452.
25. S. Kundu, M. Fowler, L. C. Simon and R. Abouatallah, *J. Power Sources*, 2008, **182**, 254-258.
26. D. Dixon, K. Wippermann, J. Mergel, A. Schoekel, S. Zils and C. Roth, *J. Power Sources*, 2011, **196**, 5538-5545.
27. L. Yang, H. Sun, S. Wang, L. Jiang and G. Sun, *J. Power Sources*, 2012, **219**, 193-198.
28. X. Cheng, C. Peng, M. You, L. Liu, Y. Zhang and Q. Fan, *Electrochim. Acta*, 2006, **51**, 4620-4625.
29. H.-Y. Jung and J.-K. Park, *Int. J. Hydrogen Energy*, 2009, **34**, 3915-3921.
30. J. Prabhuram, N. N. Krishnan, B. Choi, T.-H. Lim, H. Y. Ha and S.-K. Kim, *Int. J. Hydrogen Energy*, 2010, **35**, 6924-6933.
31. K. Yasuda, Y. Nakano and Y. Goto, *ECS Trans.*, 2007, **5**, 291-296.
32. X. Jie, Z.-G. Shao and B. Yi, *Electrochem. Commun.*, 2010, **12**, 700-702.
33. J.-Y. Park, K.-Y. Park, K. B. Kim, Y. Na, H. Cho and J.-H. Kim, *J. Power Sources*, 2011, **196**, 5446-5452.
34. J.-Y. Park, J.-H. Lee, J. Sauk and I.-h. Son, *Int. J. Hydrogen Energy*, 2008, **33**, 4833-4843.
35. J.-Y. Park, M. A. Scibioh, S.-K. Kim, H.-J. Kim, I.-H. Oh, T. G. Lee and H. Y. Ha, *Int. J. Hydrogen Energy*, 2009, **34**, 2043-2051.
36. J. Müller, in *Handbook of Fuel Cells - Vol.5/6 Advances in Electrocatalysis, Materials, Diagnostics and Durability*, eds. W. Vielstich, H. Yokokawa and H. A. Gasteiger, John Wiley & Sons, Ltd, West Sussex, 2009, vol. 6, ch. 62, pp. 916-920.
37. Y. Kim, D. Shin, J. Seo, N. Chang, H. Cho, Y. Kim and S. Yoon, *Int. J. Hydrogen Energy*, 2010, **35**, 5621-5637.
38. J. Wilhelm, H. Janßen, J. Mergel and D. Stolten, *J. Power Sources*, 2011, **196**, 5299-5308.
39. R. Kostecki, J. L. Lei, F. McLarnon, J. Shim and K. Striebel, *J. Electrochem. Soc.*, 2006, **153**, A669-A672.
40. K. A. Striebel, J. Shim, E. J. Cairns, R. Kostecki, Y. J. Lee, J. Reimer, T. J. Richardson, P. N. Ross, X. Song and G. V. Zhuang, *J. Electrochem. Soc.*, 2004, **151**, A857-A866.
41. D. P. Abraham, E. M. Reynolds, E. Sammann, A. N. Jansen and D. W. Dees, *Electrochim. Acta*, 2005, **51**, 502-510.
42. Y. Zhang and C.-Y. Wang, *J. Electrochem. Soc.*, 2009, **156**, A527-A535.
43. M. Broussely, P. Biensan, F. Bonhomme, P. Blanchard, S. Herreyre, K. Nechev and R. J. Staniewicz, *J. Power Sources*, 2005, **146**, 90-96.
44. M. Broussely, S. Herreyre, P. Biensan, P. Kaszlejna, K. Nechev and R. J. Staniewicz, *J. Power Sources*, 2001, **97-8**, 13-21.
45. M. Kerlau and R. Kostecki, *J. Electrochem. Soc.*, 2006, **153**, A1644-A1648.

46. K. Smith and C. Y. Wang, *J. Power Sources*, 2006, **160**, 662-673.
47. C. Guenther, B. Schott, W. Hennings, P. Waldowski and M. A. Danzer, *J. Power Sources*, 2013, **239**, 604-610.
48. B. Wu, V. Yufit, M. Marinescu, G. J. Offer, R. F. Martinez-Botas and N. P. Brandon, *J. Power Sources*, 2013, **243**, 544-554.
49. S. Paul, C. Diegelmann, H. Kabza and W. Tillmetz, *J. Power Sources*, 2013, **239**, 642-650.
50. Y. Zheng, L. Lu, X. Han, J. Li and M. Ouyang, *J. Power Sources*, 2013, **226**, 33-41.
51. Z.-P. Wang, P. Liu and L.-F. Wang, *Chinese Physics B*, 2013, **22**, 088801.
52. N. Cabello-Moreno, E. Crabb, J. Fisher, A. Russell and D. Thompsett, Improving the Stability of PtRu Catalysts for DMFC, Vienna, Austria, 2009.
53. J. C. Wilhelm, Ph. D. Thesis, RWTH Aachen University, 2010.
54. J. Vetter, P. Novak, M. R. Wagner, C. Veit, K. C. Moller, J. O. Besenhard, M. Winter, M. Wohlfahrt-Mehrens, C. Vogler and A. Hammouche, *J. Power Sources*, 2005, **147**, 269-281.
55. A. Barré, B. Deguilhem, S. Grolleau, M. Gérard, F. Suard and D. Riu, *J. Power Sources*, 2013, **241**, 680-689.
56. M. Dubarry, V. Svoboda, R. Hwu and B. Y. Liaw, *Electrochemical and Solid State Letters*, 2006, **9**, A454-A457.
57. Y. Chung, S. H. Ryu, J. H. Ju, Y. R. Bak, M. J. Hwang, K. W. Kim, K. K. Cho and K. S. Ryu, *Bull. Korean Chem. Soc.*, 2010, **31**, 2304-2308.